

State Space-Vector Model of Linear Induction Motors Including Iron Losses:

Part II: Model Identification and Results

Angelo Accetta, MEMBER, IEEE
National Research Council of Italy
(CNR)
Istituto di Ingegneria del Mare (INM)
Palermo, Italy
angelo.acchetta@cnr.it

Antonino Sferlazza, MEMBER, IEEE
University of Palermo
DEIM
Palermo, Italy
antonino.sferlazza@unipa.it

Maurizio Cirrincione, SENIOR MEMBER, IEEE
University of the South Pacific (USP)
School of Engineering and Physics)
Suva, Fiji
maurizio.cirrincione@usp.ac.fj

Marcello Pucci, SENIOR MEMBER, IEEE
National Research Council of Italy
(CNR)
Istituto di Ingegneria del Mare (INM)
Palermo, Italy
marcello.pucci@ieee.org

Abstract— This is the second part of a paper, divided into two parts, dealing with the definition of a space-vector dynamic model of the linear Induction motor (LIM) taking into consideration both the dynamic end-effects and the iron losses as well as the off-line identification of its parameters. This second part is devoted to the description of an identification technique which has been suitably developed for the estimation of the electrical parameters of the LIM dynamic model accounting for both the dynamic end-effects and iron losses. Such an identification technique is strictly related to the state formulation of the proposed model and exploits Genetic Algorithms (GA) for minimizing a suitable cost function based on the processing of both the primary current and speed estimation errors. The proposed parameters' estimation technique has been validated experimentally on a suitably developed test set-up. It has been further validated by a Finite Element Analysis (FEA) model of the LIM.

Keywords— *Linear Induction Motor (LIM), End-effects, Identification technique, Parameter estimation*

NOMENCLATURE

$\mathbf{u}_s = u_{sD} + j u_{sQ}$ = primary voltages space-vector in the primary reference frame;
 $\mathbf{i}_s = i_{sD} + j i_{sQ}$ = primary currents space-vector in the primary reference frame;
 $\mathbf{i}'_r = i_{rd} + j i_{rq}$ = secondary currents space-vector in the primary reference frame;
 $\boldsymbol{\psi}_s = \psi_{sD} + j \psi_{sQ}$ = primary flux space-vector in the primary reference frame;
 $\boldsymbol{\psi}'_r = \psi_{rd} + j \psi_{rq}$ = secondary flux space-vector in the primary reference frame;
 L_s, L_r, L_m = primary, secondary and three-phase magnetizing inductances;
 $L_{\sigma s}, L_{\sigma r}$ = primary and secondary leakage inductances;
 R_s, R_r = primary and secondary resistances;
 p = number of pole pairs;
 ω_r = angular rotor speed (in electrical angles per second);

v = linear speed;
 τ_m = length of the primary;
 τ_p = polar pitch.

I. INTRODUCTION

This is the second part of a paper, divided into two parts, dealing with the definition of a space-vector dynamic model of the linear Induction motor (LIM) taking into consideration both the dynamic end-effects and the iron losses and its off-line identification. The first part has treated the theoretical framework of the model [1]. This second part, that recalls briefly the equations of the model, is mainly devoted to the description of an identification technique, which has been suitably developed for the estimation of the electrical parameters of the LIM dynamic model described in [1]. From the point of view of the LIM dynamic modelling, [1] represents an upgrade and evolution of [2], that defined a dynamic model able to take into account the LIM dynamic end-effects, but not for the iron losses. As for the identification techniques of Rotating Induction Motors (RIM), the scientific literature is huge, ranging from traditional no-load and locked rotor tests to more sophisticated dynamical tests [3]-[9]. In general, two approaches have been followed to solve this problem. The first one permits the direct computation of some electrical parameters starting from the measurements of the input voltages and currents; such measurements are further elaborated by either spectral analysis, or linear or non-linear regression techniques [5][6]. The second one permits the machine parameters to be estimated, starting from the construction of suitable state observers (full-order or reduced-order observers, extended Kalman filter, model reference adaptive systems). In this case, the accuracy of the state reconstruction depends on the adaptive estimation of a suitably chosen set of electrical parameters. The correct set of parameters is the one permitting the best fitting between the output computed by the dynamic model and that coming from the real machine.

It should be noted, however, that there is a consistent difference between LIMs and RIMs, as for the parameters estimation methodologies. Firstly, the traditional no-load and

locked tests cannot be easily performed in *LIMs*. As a matter of fact, while the locked primary test can be performed on the one hand, because the primary can be locked in its position, on the other hand the no-load test can be hardly performed. This is due to the limited length of the secondary track, which can prevent the steady-state rated speed to be reached. In addition, any no-load test made in absence of the secondary would unavoidably lead to a wrong parameter estimation, because of the significant modification of the structure of the machine magnetic circuit. Last but not least, the tests traditionally devised for *RIMs* cannot permit the additive terms of the equivalent circuit considering the end-effects to be computed. In this respect, only dynamical tests can be envisaged in *LIMs*.

As for the scientific literature, very few papers specifically treat the identification of *LIMs* parameters [10]-[17]. Some of them specifically face up to the dynamic or static modelling of the *LIM*, to be used for solving the identification problem. For example, [15] proposes a dynamic model of the *LIM* considering the actual winding distribution and structure dimensions. It can calculate the mutual, self, and leakage inductance to describe the influence of the longitudinal end-effects and half-filled slots. [13] specifically deals with some issues related to the *LIM* modelling, involving the transversal edge and longitudinal end-effects and the half-filled slots at the primary. It finally come up with the definition of a T-model equivalent circuit based on the 1-D magnetic equations of the air gap. [14] focuses an improved series equivalent circuit for this machine, where the longitudinal end-effects are estimated using three different impedances representing the normal, the forward, and the backward flux density waves in the air gap.

[16] proposes an on-line model reference adaptive system (*MRAS*) exploited for simultaneously estimating the secondary resistance and the three-phase magnetizing inductance. The drawbacks of such an approach is the adoption a force formulation not accounting the braking component caused by end-effects.

Among the most significant papers, there is certainly [11]. In [11], the parameters of the equivalent steady-state circuit of a *RIM* are computed by means of a Finite Element Analysis (*FEA*) of the linear motor; in particular, the leakage inductances of the primary and the secondary are estimated by flux analysis with a *FEA*. To do that, the primary and the secondary are supplied separately by current waveforms. The obtained data are processed and, afterwards, the *RIM* model is exploited. Such a work presents three weaknesses: 1) it does not find the *LIM* parameters considering either the border or the end-effects, 2) it necessarily requires the *FEA*, with the consequent limitations (for example, the geometrical and constructional data of the motor are not always available to the final user), 3) the operating conditions in which the leakage inductances are estimated are very different from real ones, with resulting potential significant estimation errors.

All the above considerations call, from one side, for a proper dynamical model of the *LIM* taking in to consideration at the same time both the dynamic end-effects and the iron losses, and, from the other side, a suitable methodology for the identification of its parameters; such a methodology should hopefully exploit just input voltage/current measurements, not necessarily requiring

either the constructional data of the *LIM* nor any complex *FEA*.

The approach proposed in this paper can be viewed as an extension of the parameters' estimation technique for *LIMs* proposed in [17], with respect to which several improvements are introduced here. In particular, while [17] had been specifically devised to estimate the electrical parameters of the model proposed in [2], the methodology proposed here has been conceived to estimate the electrical parameters of the model proposed in [1]. The difference lies in the dynamic model of the *LIM* whose parameters have to be estimated. Specifically, while the model in [2] presents 4 scalar electrical variables, the model in [1] presents 6 scalar electrical variables. Correspondingly, the set of electrical parameters to be estimated has been modified with respect to [17]. In particular, the following set of electrical parameters has been estimated here: primary inductance (L_s), global leakage inductance (σL_s), secondary resistance (R_r), iron losses resistance (R_θ). A specific dynamic test has been conceived in this paper, permitting all the above electrical parameters to be estimated after processing off-line the data acquired during it. Specifically, the proposed parameters estimation technique exploits the Genetic Algorithms (*GA*) [18] for minimizing a suitable cost function, processing the weighted sum of the error between the measured primary current and its estimation obtained on the basis of the proposed model as well as the error between the experimental measured linear speed and its estimation obtained on the basis of the model in [1]. After having estimated the complete set of electrical parameters of the *LIM* on the basis of the proposed *GA* approach, the goodness of the solution has been further verified comparing the results achievable with the proposed *LIM* model with those obtained with the *FEA*. With this specific regard, the complete *FEA* model of the *LIM* under test has been developed by the authors in *Flux-2D*[®] environment.

II. SPACE VECTOR MODEL OF THE LIM INCLUDING IRON LOSSES

In the following, the dynamic model of the *LIM* including the iron losses is briefly described. For the details related to the model, the reader can refer to [1].

Starting from the space-vector electric scheme in Fig. 1, the following space-vector voltage equations can be written on the primary (a) and secondary (b) circuits:

$$\begin{aligned} \mathbf{u}_s &= R_s \mathbf{i}_s + \hat{R}_r \mathbf{i}_m + \frac{d\boldsymbol{\psi}_s}{dt} = R_s \mathbf{i}_s + \hat{R}_r [\mathbf{i}_s + \mathbf{i}'_r - \mathbf{i}_0] + \frac{d\boldsymbol{\psi}_s}{dt} \\ \mathbf{u}'_r &= R_r \mathbf{i}'_r + \hat{R}_r \mathbf{i}_m + \frac{d\boldsymbol{\psi}'_r}{dt} - j \omega_r \boldsymbol{\psi}'_r \end{aligned} \quad (1 \text{ a, b})$$

For the meaning of symbols, the reader can refer to nomenclature at the beginning of the paper. For the meaning of the time-varying parameters of the *LIM* due to the end effects, the reader can refer to [2].

Eq.s (1 a, b) have been written exploiting the following current balance equation at the node:

$$\mathbf{i}_s + \mathbf{i}'_r = \mathbf{i}_m + \mathbf{i}_0 \quad (2)$$

Eq.s (6 a, b) are different from both the equations of the *LIM* accounting for the end-effects and those of the *RIM* including the iron losses. With respect to the *RIM* model including the iron losses, they include the voltage drop on

the variable resistance \hat{R}_r due to the magnetizing current \mathbf{i}_m . The flux equations can be written as:

$$\begin{aligned}\psi_s &= L_{\sigma s} \mathbf{i}_s + \hat{L}_m \mathbf{i}_m = L_{\sigma s} \mathbf{i}_s + \psi_m \\ \psi_r &= L_{\sigma r} \mathbf{i}_r + \hat{L}_m \mathbf{i}_m = L_{\sigma r} \mathbf{i}_r + \psi_m\end{aligned}\quad (3 \text{ a, b})$$

A further equation, not present either in classic *RIM* model or in the *LIM* model accounting for the end-effects, is the voltage equation across R_0 :

$$\frac{d\psi_m}{dt} + \hat{R}_r \mathbf{i}_m = \frac{d\psi_m}{dt} + \frac{\hat{R}_r}{\hat{L}_m} \psi_m = R_0 \mathbf{i}_0 \quad (4)$$

As for the state representation of the above described model, the reader can refer to [1].

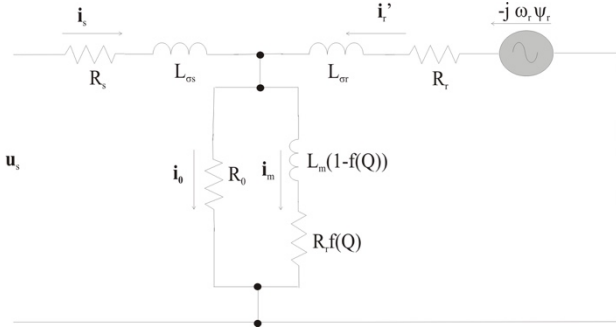


Fig. 1. Space-vector equivalent circuit of the LIM including dynamic end effects and iron losses

III. LIM PARAMETERS' ESTIMATION

As for the traditional dynamic model of the RIM, it is well known that not all the components of the state are measurable quantities. In particular, if the RIM model involving the stator currents and the rotor fluxes as state variables, the direct and quadrature components of the stator currents are the part of the state which is measurable, while the corresponding components of the rotor flux are the part of the state which is not measurable. As a direct consequence, only a limited number of the RIM electrical parameters can be estimated exploiting input-output measurements. This set of parameters can be suitably identified adopting convenient numerical techniques as in [3]-[9].

As for the RIM model identifiability conditions, it is well known that the full set of 4 electrical parameters (stator resistance, stator inductance, global leakage factor, rotor time constant) can be identified only exploiting a full speed transient of the machine. On the contrary, in sinusoidal steady-state condition, only 1 electrical parameter can be computed. This issue, known as the rank deficient problem, can be viewed from several points of view.

Firstly, if the RIM equations are rewritten in terms only of the input-output measurable quantities, stator current and voltage space vectors, then the parameter estimation problem can be formalized as a linear regression one [5]-[6]. Reading such papers, it is clear that the computation of all the parameters, from which the electrical ones can be deduced, requires at least 2 measurements of speed;

otherwise, at any constant speed, the rows of the data matrix are linearly dependent. Such an observation is coherent with the evidence that just two tests can be classically exploited, the no-load and the locked rotor tests, to retrieve the same parameters at sinusoidal steady-state with just two tests performed at two different speeds: no load synchronous speed and zero speed.

Finally, the same problem can be faced up from the point of view of the observability. The RIM model is observable starting from the measurements of the speed and the stator current, for all the applied voltages. It implies that the full system dynamics is observable by the input-output measurements and therefore a unique set of parameters exists reproducing both the input-output behaviour as well as the state dynamics. All these considerations which are valid for RIMs, can be easily extended to LIMs without any loss generality.

From a theoretical point of view, therefore, a set of very few measurements performed at different speed would be sufficient to estimate the entire set of 4 electrical parameters. From a practical point of view, however, if a bigger set of input-output measurement is recursively elaborated, a natural filtering occurs leading naturally to the retrieval of the best solution. An entire speed transient from zero speed to the steady-state speed is further suggestible, since it permits the values of the electric parameters corresponding to the steady-state magnetization of the RIM to be retrieved [6]. Such an approach, developed in [6] for the RIMs has been suitably extended to LIMs in [25], where an algorithm based on the minimization of a suitable cost function involving the differences of the measured primary current components and those computed by simulation, has been adopted. Under such an assumption, an estimate of the variation of the electric parameters of the LIM with the magnetizing current has been obtained, as shown in [17]. It should be noted that the model adopted in [17] for the parameters' estimation is the dynamic model accounting for the dynamic end-effects proposed in [1].

On the contrary, in this paper, the new dynamic model of the LIM has been adopted, accounting for both the dynamic end-effects and iron losses; the theoretical description of this is written in [1]. Since the state representation of the LIM, because of the presence of the iron losses changes, as clearly described in [1], leading to an increased number of the state variables from 4 scalar to 6 scalar, correspondingly even the number of electrical parameters to be estimated varies, including the iron losses resistance R_0 , which was not accounted in [17].

In this paper, the stator resistance R_s is not assumed as a quantity to be estimated by the proposed technique, since it can be easily measured with simple voltage/current measurements. Therefore, the model presented in [1] can be expressed as function of the following vector β , representing the set of the electrical parameters to be estimated:

$$\beta = [\sigma L_s \quad L_s \quad R_r \quad R_0]^T \quad (5)$$

In order to identify the vector of the parameters β of the model (1)-(4), a suitable optimization problem can be considered. The LIM has been supplied in order to perform a set of speed transients; in correspondence to each value of speed steady-state, several load forces have been given to the LIM drive. In this way, the working space composed of

speed and load forces can be suitably covered for parameter estimation. The primary voltages and currents, the load force and the linear speed acquired during the above tests have been recorded. Afterwards, the space-vector state model (1)-(4) has been supplied numerically with the same values of primary voltages adopted in the experimental test, and the primary currents and the speed have been computed by the model (1)-(4). Finally, the difference between the measured primary currents and speed and the corresponding ones estimated by the model have been exploited to recursively tune the values of the model's parameters, until when the outputs of the model match the corresponding ones of the real LIM. Note that the speed depends from the electromagnetic force generated by the motor, therefore the use of this variable for estimating the model parameters is very important because it takes into account the effective magnetization level of the machine, since the force depends both from primary currents and secondary flux. Fig. 2 sketches the block diagram of the technique adopted for the parameter estimation of the LIM. As for the tuning algorithm, the optimization problem has been formulated as follows:

$$\min_{\beta} S(\beta) \quad \text{subject to:} \quad (6)$$

$$L_{\beta_i} \leq \beta_i \leq U_{\beta_i} \quad i = 1, 2, 3, 4.$$

where β is the vector of parameters (5), L_{β_i} and U_{β_i} are the lower and upper bounds of each parameter β_i respectively and they are introduced in order to restrict the searching domain and avoid to look for negative parameters or parameters without physical meaning, and $S(\beta)$ is the cost function defined as follows:

$$S(\beta) = \frac{1}{N} \sqrt{\alpha_1 \sum_{k=1}^N \left((i_{sD}(k) - \widehat{i_{sD}}(k))^2 + (i_{sQ}(k) - \widehat{i_{sQ}}(k))^2 \right) + \alpha_2 \sum_{k=1}^N (v(k) - \widehat{v}(k))^2} \quad (7)$$

where N is the total number of samples taken into consideration by the algorithm, k is the discrete instant of time, i_{sD} and i_{sQ} are the vectors of the measured direct and quadrature primary currents, $\widehat{i_{sD}}$ and $\widehat{i_{sQ}}$ are the corresponding quantities computed by means of the mathematical model in eq. (1)-(4) adopting the values of the parameters (5) under the same supply voltage, v and \widehat{v} are respectively the measured linear velocity of the LIM and the estimated one. Finally, α_1 and α_2 are two positive weighting constants, allowing to separately weight the primary current and speed errors. With respect to [17], therefore, an additional term has been considered in the cost function, accounting for the balance between the real propulsive force and that estimated by the model. This has been necessary since the parameter R_0 accounts for iron losses, depending on the supply frequency of the machine and therefore on its speed.

Finally, the solution of the identification problem is the vector:

$$\beta^* = \arg \min_{\beta} S(\beta) \quad (8)$$

of the parameters solving the problem in eq. (6).

Now the problem is how to find the optimum β^* , since problem (6)-(8) is a non-linear and non-convex problem, so the standard linear techniques do not ensure the optimal solution. In order to solve the problem, in the case under study, the genetic algorithms have been used, because they are very suitable for solving this type of problems. Actually, it is well known, the genetic algorithm starts from a generic initial condition, that is an initial population of individuals randomly generated into the domain defined by the lower and upper bounds L_{β_i} and U_{β_i} , and it is quite robust versus this initial condition choice; thus, whatever the initial condition is, the GA will converge towards the global minimum.

The genetic algorithm generates a set of parameters β (i.e. one β for each individual) so that the algorithm can calculate the $S(\beta)$ associated with each β . Each individual is evaluated by a fitness function and the genetic algorithm selects the best parameter β and generates a new set of parameters β as new generation (inside the domain generated by the lower and upper bounds L_{β_i} and U_{β_i}). Several genetic operators have been applied to produce a new generation of β , each new generation overlaps the previous generation of β . The cycle is iterative until a predefined stopping criterion is met. In particular the algorithm is stopped when a predefined number of generations is reached or is the cost function $S(\beta)$ is lower than a certain threshold.

With reference to the other GA tuning parameters, the following choice has been made: a) mutation function: constraint dependent; b) crossover function: scattered; c) selection function: stochastic uniform; d) elite count: 5% of the population size; e) crossover fraction: 0.8. See [18] for details about the use of the genetic algorithms.

Moreover, another purposely devised method has been used during the identification procedure. In particular, for both approaches, some parameters have been normalized by means of constant scalars so that all parameters range in comparable sets of values. In particular the following rescaled vector has been used instead of (5):

$$\bar{\beta} = [30 \cdot \sigma L_s \quad 10 \cdot L_s \quad R_r/10 \quad R_0/10]^T \quad (6)$$

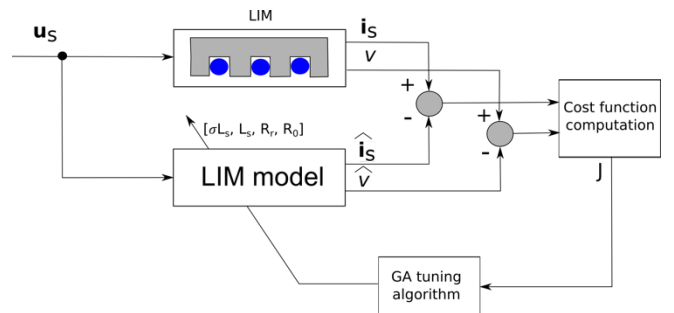


Fig. 2. Block diagram of the identification scheme of the LIM

With choice (6) the following upper and lower bounds L_{β_i} and U_{β_i} have been selected:

$$L_{\beta_i} = [1 \quad 2 \quad 1 \quad 5],$$

$$U_{\beta_i} = [10 \quad 10 \quad 6 \quad 20],$$

and the two positive weighting constants α_1 and α_2 have been selected equal to: $\alpha_1 = 1$ and $\alpha_2 = 3$.

The number of individuals chosen in this application is 50, while the stopping criteria has been selected equal to 50 iterations which corresponds with the number of epochs.

From the experimental results shown in the next section it will be shown that the above described procedure leads to a good choice of the model's parameters ensuring a small value of the cost function (7).

IV. TEST SET-UP

A test set-up has been suitably built to verify the parameters' estimation technique proposed in this paper. The machine under test is a LIM model Baldor LMAC1607C23D99, whose rated data and electrical parameters are shown in Tab. I. The LIM has been equipped with a linear encoder Numerik Jena LIA series. The LIM presents a secondary track whose length is 1.6 m.

The employed test set up consists of:

- A three-phase linear induction motor with parameters shown in Table I;
- A frequency converter which consists of a three-phase diode rectifier and a 7.5 kVA, three-phase VSI;
- A dSPACE card (DS1103) with a PowerPC 604e at 400 MHz and a floating-point DSP TMS320F240.

The test set-up is equipped also with a torque controlled PMSM (Permanent Magnets Synchronous Motor) model Emerson Unimotor HD 067UDB305BACRA mechanically coupled to the LIM by a pulley-strap system, to determine an active load for the LIM. Fig. 3 shows a photograph of the test set-up.



Fig. 3. Photograph of the experimental test set-up

TABLE I. PARAMETERS OF THE LIM

Rated power P_{rated} [W]	424.7
Rated voltage U_{rated} [V]	380
Rated frequency f_{rated} [Hz]	60
Pole-pairs	3
Inductor resistance R_s [Ω]	11
Inductor inductance L_s [mH]	698
Induced part resistance R_r [Ω]	28.36
Induced part inductance L_r [mH]	716.3
3-phase magnetizing inductance L_m [mH]	680
Rated thrust F_n [N]	200
Rated speed [m/s]	6.85
Mass [kg]	20

V. EXPERIMENTAL RESULTS

The proposed parameters' estimation technique of the LIM model taking into consideration both the dynamic end-effects and the iron losses has been experimentally validated on the test set-up described in Section IV. Moreover, it has been further verified comparing its results with those obtained with finite element analysis (FEA) tests. In the experimental test the LIM drive has been run with a FOC algorithm so that closed loop control of the LIM speed and induced part flux amplitude has been performed [19].

The parameters of the model in [1] have been identified adopting the technique described in Section III. In the following figures, the quantities estimated are referred to the results obtained in numerical simulation adopting the proposed model whose parameters represent the final values of the estimated parameters, at the end of the identification process.

A. Experimental Validation

A set of speed step references ranging between 0.1 m/s and 0.8 m/s with several speed reversals has been imposed the LIM drive. Correspondingly, a set of step load forces has been applied by setting a priori a load force pattern to be given to the torque controlled PMSM drive used as active load.

Fig. 4 shows the LIM experimental speed and that computed by the proposed model during the performed test. It can be seen that the LIM drive is able to correctly track any variation of the reference speed. Moreover, at each speed, it is visible that there are some instants in which the load force is applied and therefore the speed control loop reacts to the load application.

The speed waveform computed by the proposed model correctly matches the corresponding measured experimentally, even during the speed transients arising from the application of the load force, as confirmed by the speed estimation error trace.

Figs 5 and 6 show, in the upper subplot, the corresponding waveforms of the i_{sD} , i_{sQ} primary current components, expressed in the primary reference frame. The same figures, in the lower subplot, show also the corresponding current estimation errors, meaning the instantaneous differences between the measured currents and those computed by the proposed model. Even for these figures, it can be noted a very good matching between the instantaneous measured primary current and the corresponding ones computed by the proposed model. Such consideration is confirmed by the instantaneous error curve, which is always in average equal to zero and instantaneously never exceeding 5% (please mind that these are errors on AC quantities, thus even a small time lag can cause a significant estimation error). Fig. 7 shows the corresponding waveforms of the three-phase magnetizing and secondary flux amplitudes (upper subplot) and the net electromagnetic force (difference between the propulsive force and the end-effects braking force), while Fig. 8 shows the load force waveform, as applied by the PMSM torque controlled drive used as active load. Even in this case, the net force computed by the model correctly

matches the experimental one. With this specific regard, as specified above, even the experimental net force is an estimated quantity.

Figs 9 and 10 show respectively the estimated values of σL_s , L_s , R_r and R_θ versus the number of iterations during the identification process. To make the identification transient more readable only the first 25 iterations have been shown even if the entire identification process has been shown at 50th. It can be noted that after almost 15 iterations the algorithm converges to the final solution. The goodness of the identification process is indirectly demonstrated by the correct machine between the estimated and experimentally acquired state variable (See Figs 4-7), and directly by the cost function values versus iterations shown in Fig. 11. It can be noted that such cost function converges to its minimum.

The solution of the identification process has provided the following parameter vector:

$$\beta^* = [0.053 \quad 0.698 \quad 28.36 \quad 145.7]^T$$

and the associated cost function value is: $S(\beta^*)$ 0.0612.

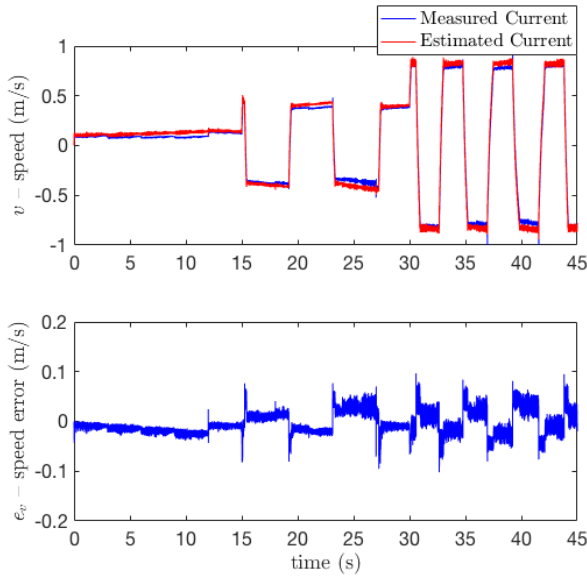


Fig. 4. LIM linear speed and speed estimation error– experiment vs model

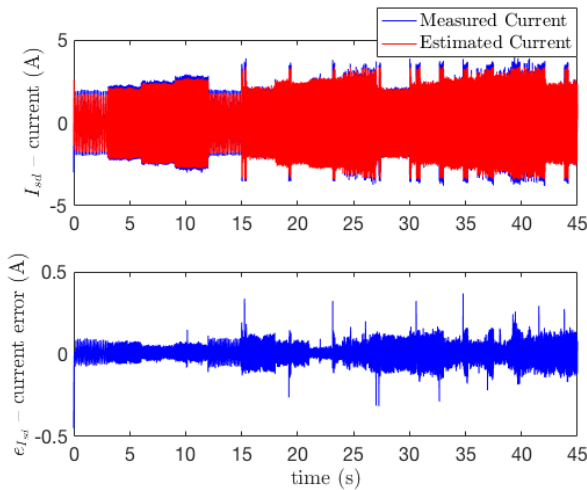


Fig. 5. LIM i_{sd} current and estimation error – experiment vs model

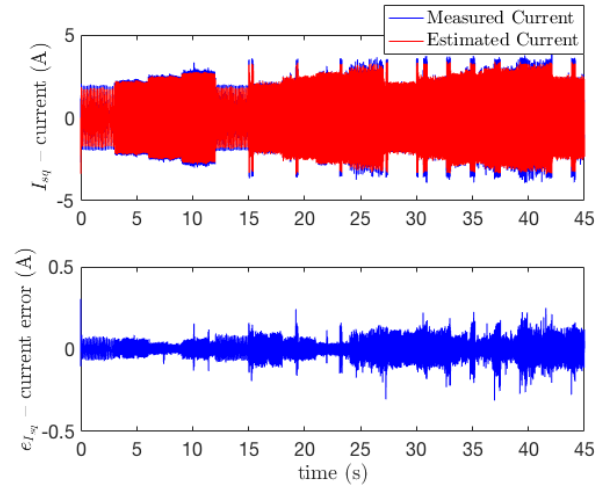


Fig. 6. LIM i_{sq} current and estimation error – experiment vs model

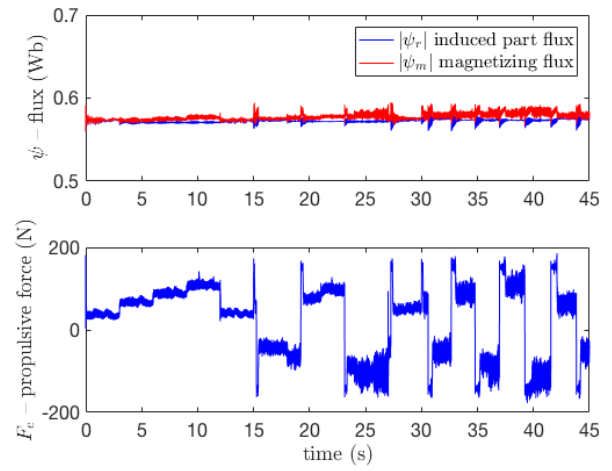


Fig. 7. LIM induced part flux amplitude and net force – experiment vs model

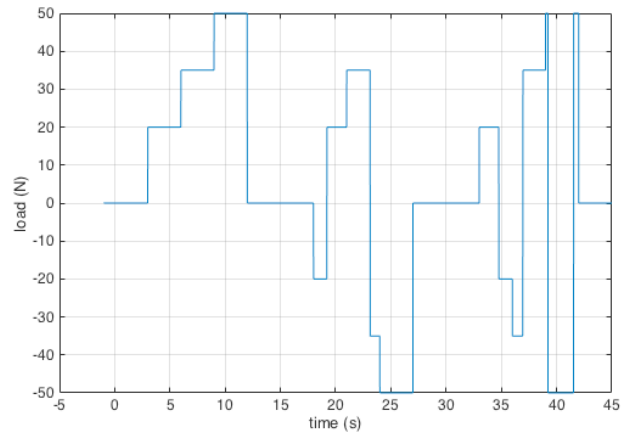


Fig. 8. LIM load force – experiment

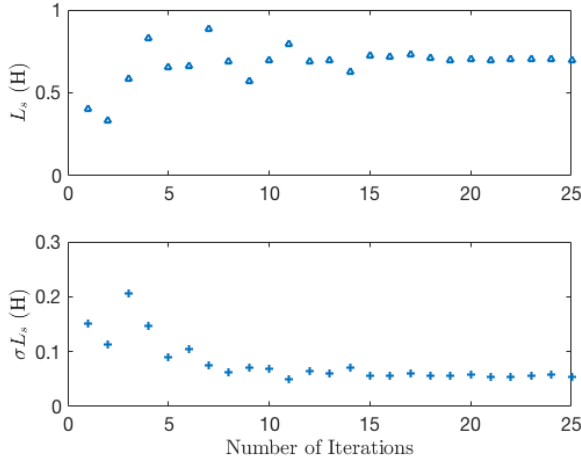


Fig. 9. Estimated L_s and σL_s vs number of iterations – experiment

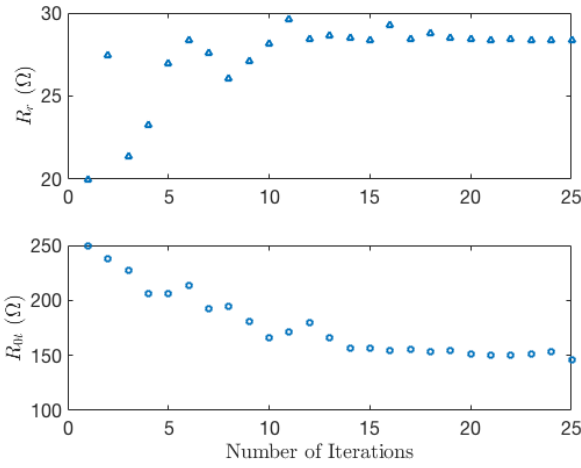


Fig. 10. Estimated R_r and R_0 vs number of iterations – experiment

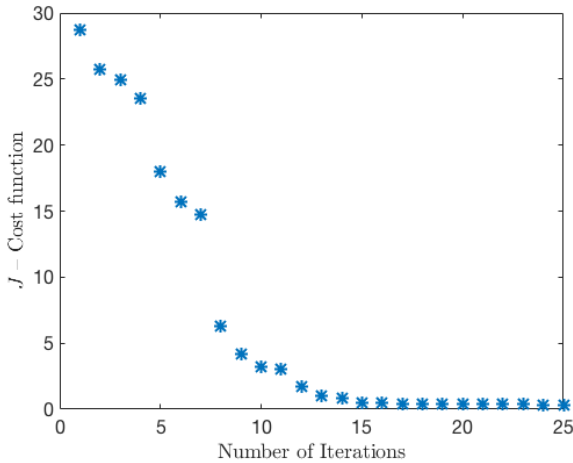


Fig. 11. Fitness function versus number of generations during the parameters' estimation test

B. FEA Validation

After having identified the parameters of the proposed model on the basis of the above described experimental

tests, the proposed identification technique has been verified also comparing its results with those obtainable with the *FEA* model of the machine under test. The *LIM* under tests has been modelled by the *FEA* software *FLUX-2D*[®]. Currently, only a 2D transient analysis has been performed. With this specific regard, Fig. 12 shows the longitudinal *CAD* cross-section of the *LIM* under test, as utilized for running the *FEA*, highlighting also the positioning in the primary core of the phase windings. Fig. 13 show the flux density contour lines at steady-state obtained as the result of *FEA*.

With the aim of validating the proposed model also by *FEA*, the following test has been made. A start-up test has been performed at the supply voltage of 260 V RMS with frequency equal to 60 Hz. All the following figures plot, on the same graph, the quantity computed with the proposed model and the quantity computed by the *FEA*. Figs. 14, 15, 16, 17 show respectively the *LIM* speed, the i_{sD} , i_{sQ} primary current components with the corresponding current estimation error, the secondary flux amplitude and net force. It can be seen that the all the quantities computed with the proposed model are very close to the corresponding estimated by *FEA*. The speed, the secondary flux and the force waveforms computed by the proposed model are perfectly superimposed to the *FEA* curves. Even the primary currents present very small estimation errors, which can be considered negligible.

Finally, Fig. 18 shows the 3-D plot of the corresponding flux density contour versus time and the linear position of the inductor.

The comparison between the results obtained from one side with the proposed model whose parameters have been retrieved with above described parameters' estimation technique and from the other side with *FEA* permits a definitive validation of both the proposed model and the related identification procedure.

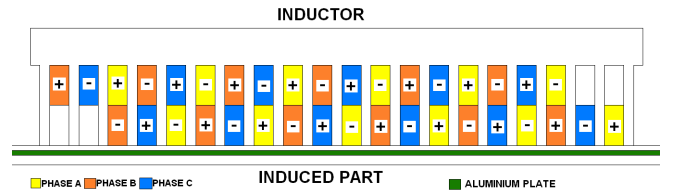


Fig. 12. CAD sketch of the LIM under test

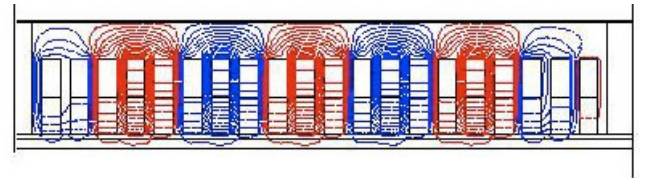


Fig. 13. Flux density contour lines at steady-state

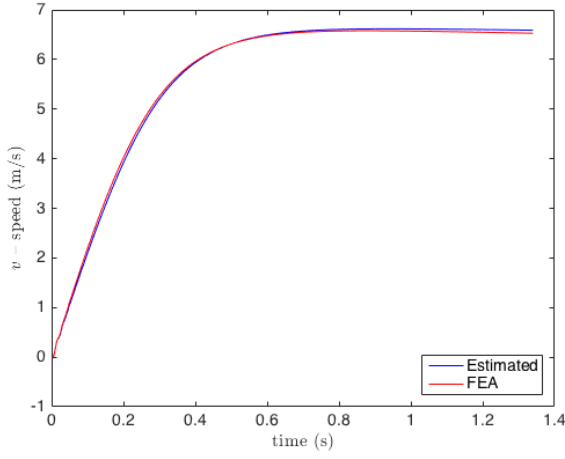


Fig. 14. LIM linear speed – FEA vs proposed model

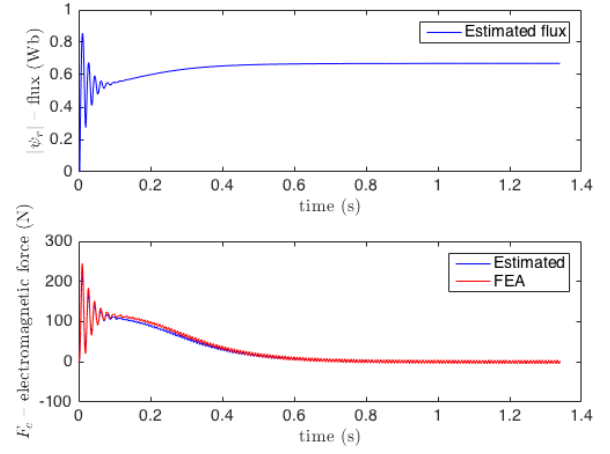


Fig. 17. LIM secondary flux amplitude and net force – FEA vs proposed model

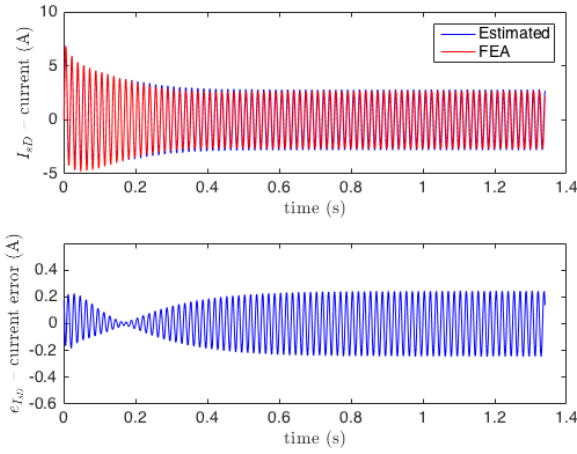


Fig. 15. LIM i_{sD} current and corresponding estimation error – FEA vs proposed model

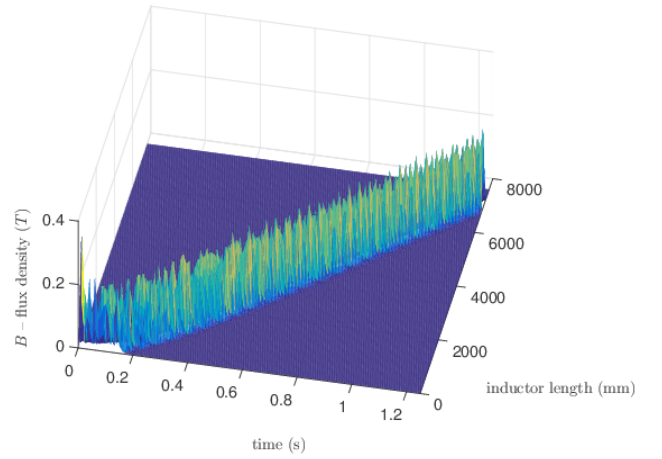


Fig. 18. flux density versus time and primary position obtained with FEA

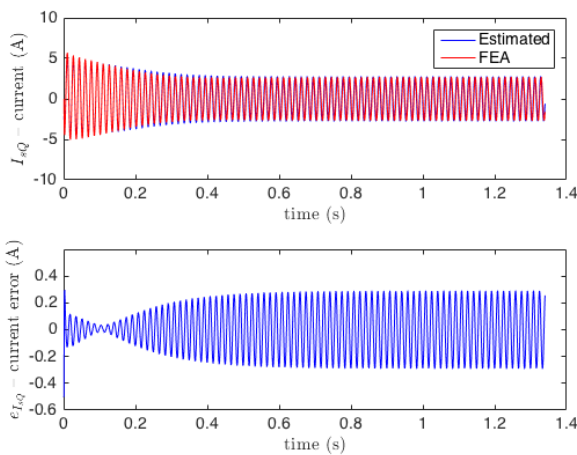


Fig. 16. LIM i_{sQ} current and corresponding estimation error – FEA vs proposed model

Such an identification technique is strictly related to the state formulation of the proposed model and exploits Genetic Algorithms (GA) for minimizing a suitable cost function. The proposed dynamic model and its related parameters estimation technique have been validated comparing its results with those obtainable experimentally on a suitably developed test set-up and with those obtainable by a FEA model of the LIM.

VI. CONCLUSIONS

This paper proposes a parameter estimation technique developed to identify the electrical parameters of the dynamic model of the linear induction motor taking into consideration both end-effects and iron losses. The proposed technique is based on GA and minimizing a suitably conceived cost function depending on the weighted sum of the primary current and speed errors. The proposed method has been validated firstly on the experimentally developed test set-up and secondly on the FEA model. The results

show the effectiveness of the proposed method and the correctness of the estimated parameters.

REFERENCES

- [1] A. Accetta, M. Cirrincione, M. Pucci, A. Sferlazza, "State Space-Vector Model of Linear Induction Motors Including Iron Losses Part I: Theoretical Analysis", *IEEE Energy Conversion Congress and Expo 2018 (ECCE 18)*, 23-27 September 2018, Portland, USA.
- [2] M. Pucci, "State space-vector model of linear induction motors," *IEEE Transactions on Industry Applications*, vol. 50, no. 1, pp. 195–207, 2014.
- [3] H. A. Toliyat, E. Levi, M. Raina, "A review of RFO induction motor parameter estimation techniques", *IEEE Power Eng. Rev.*, Vo. 22 , n. 7, 2002.
- [4] H. A. Toliyat, E. Levi, M. Raina, "A review of RFO induction motor parameter estimation techniques", *IEEE Trans. on Ener. Conv.*, Vol. 18 , n. 2, pp. 271 – 283, 2003.
- [5] M. Cirrincione , M. Pucci , G. Cirrincione , G. A. Capolino, " A New Experimental Application of Least-Squares Techniques for the Estimation of the Induction Motor Parameters", *IEEE Transactions on Industry Applications*, vol.39, n.5, September/October 2003, pp.1247-1256
- [6] M. Cirrincione, M. Pucci, G. Cirrincione, G. Capolino, "Constrained Minimisation for Parameter Estimation of Induction Motors in Saturated and Unsaturated Conditions ", *IEEE Transactions on Industrial Electronics*, Vol. 52, n. 5, Oct. 2005, pp. 1391 – 1402
- [7] M. H. Haque, "Determination of NEMA Design Induction Motor Parameters From Manufacturer Data", *IEEE Transactions on Energy Conversion*, vol. 23, n. 4, 2008 , pp. 997-1004.
- [8] A. Boglietti, A. Cavagnino, M Lazzari, "Computational Algorithms for Induction-Motor Equivalent Circuit Parameter Determination—Part I: Resistances and Leakage Reactances", *IEEE Transactions on Industrial Electronics*, vol. 58, n. 9, 2011, pp. 3723- 3733
- [9] A. Boglietti, A. Cavagnino, M Lazzari, "Computational Algorithms for Induction Motor Equivalent Circuit Parameter Determination—Part II: Skin Effect and Magnetizing Characteristics", *IEEE Transactions on Industrial Electronics*, vol. 58, n. 9, 2011, pp. 3734-3740.
- [10] Gubae Kang; Junha Kim; Kwanghee Nam, "Parameter estimation of a linear induction motor with PWM inverter", *The 27th Annual Conference of the IEEE Industrial Electronics Society, 2001. IECON '01*, vol. 2, 2001, pp. 1321- 1326
- [11] Gubae Kang, Junha Kim, Kwanghee Nam, "Parameter estimation scheme for low-speed linear induction motors having different leakage inductances", *IEEE Trans. on Ind. Electr.*, vol. 50, n. 4, 2003, pp. 708 – 716.
- [12] Liming Shi; Ke Wang; Yaohua Li, "On-line parameter identification of linear induction motor based on adaptive observer", *International Conference on Electrical Machines and Systems, 2007. ICEMS, 2007*, pp. 1606-1609.
- [13] W. Xu, J. Zhu, Y. Zhang, Z. Li, Y. Li, Y. Wang, Y. Guo and Y.J. Li, "Equivalent circuits for single-sided linear induction motors," *IEEE Transactions on Industry Applications*, vo.46, no.6, pp.2410-2423, Nov./Dec. 2010.
- [14] W. Xu, J. Zhu, Y. Zhang, Y. Li, Y. Wang, and Y. Guo, "An improved equivalent circuit model of a single-sided linear induction motor," *IEEE Transactions on Vehicular Technology*, vol.59, no.5, pp.2277-2289, Jun. 2010.
- [15] W. Xu, G. Sun, L. Wen, W. Wu, and P. Chu, "Equivalent circuit derivation and performance analysis of a single-sided linear induction motor based on the winding function theory," *IEEE Transactions on Vehicular Technology*, vol.61, no.4, pp.1515-1525, May 2012.
- [16] Z. Zhang, T. R. Eastham, G. E. Dawson, "Peak thrust operation of linear induction machines from parameter identification", *Conference Record of the 1995 IEEE Industry Applications Conference, 1995. Thirtieth IAS Annual Meeting, IAS '95, 1995*, pp. 375-379.
- [17] F. Alonge, M. Cirrincione, F. D'Ippolito, M. Pucci, and A. Sferlazza, 653 "Parameter identification of linear induction motor model in extended 654 range of operation by means of input-output data," *IEEE Transactions on Industry Applications*, 655 vol. 50, no. 2, pp. 959–972, Mar./Apr. 2014.
- [18] M. Gen and R. Cheng, *Genetic Algorithms and Engineering Optimization*, New York: Wiley, 2000.
- [19] M. Pucci, "Direct field oriented control of linear induction motors," *Elect. Power Syst. Res.*, vol. 89, pp. 11–22, 2012.